New Class of Hole-Blocking Amorphous Molecular Materials and Their Application in Blue-Violet-Emitting Fluorescent and Green-Emitting Phosphorescent Organic Electroluminescent Devices

Kenji Okumoto and Yasuhiko Shirota*

Department of Applied Chemistry, Faculty of Engineering, Osaka University, Yamadaoka, Suita, Osaka 565-0871, Japan

Received August 19, 2002. Revised Manuscript Received December 6, 2002

A new class of hole-blocking amorphous molecular materials for use in organic electroluminescent (EL) devices have been developed, which include 1,3,5-tri(4-biphenylyl)benzene, 1,3,5-tris(4-fluorobiphenyl-4′-yl)benzene (F-TBB), 1,3,5-tris(9,9-dimethylfluoren-2-yl)benzene, and 1,3,5-tris[4-(9,9-dimethylfluoren-2-yl)phenyl]benzene. They readily form stable amorphous glasses with well-defined glass-transition temperatures and are characterized by relatively high oxidation potentials and large HOMO−LUMO energy gaps. The use of these materials as hole blockers enabled blue-violet emission from several emitting amorphous molecular materials with hole-transporting properties in organic EL devices. A multilayer organic EL device using *N*,*N*-bis(9,9-dimethylfluoren-2-yl)aniline (F_2PA) as a blue-violet emitter, F-TBB as a hole blocker, and 4,4′,4″-tris[3-methylphenyl(phenyl)amino]triphenylamine and tris(8-quinolinolato)aluminum as hole and electron transporters, respectively, exhibited blue-violet emission peaking at 405 nm with a high external quantum efficiency of 1.95%. This device also enabled the doping of a phosphorescent iridium complex, tris(2-phenylpyridine)iridium ($Ir(ppy)_3$), tuning the emission color from blue violet to green by excitation energy transfer from F_2PA to $Ir(ppy)_3$.

Introduction

Organic electroluminescent (EL) devices permit emission of various colors depending upon emitting materials. Among them, blue-emitting organic EL devices have been a subject of current interest.[1−18] It is also a subject of great interest and significance to develop devices that emit light of shorter wavelengths, i.e., blue-violet to violet light, because such devices can be utilized to generate light of various colors either by irradiation of luminescent dyes or by excitation energy transfer to luminescent dopants including emissive phosphors.

Up to now, there have been only several reports on blue-violet-emitting organic EL devices that emit light peaking at wavelengths shorter than 420 nm. The reported devices exhibit low performance with high turn-on voltages, low quantum efficiencies, and low luminances. The devices using polysilanes emit light peaking at 405 nm, but the turn-on voltage is as high as 8 V and the external quantum yield is only 0.2%.[19] The devices using poly(*N*-vinylcarbazole) and *N*,*N*′-diethyl-3,3′-bicarbazole emit light peaking at 410 and 415 nm, but the luminance is low, being 700 cd m^{-2} at 14 V and 20 cd m^{-2} at 250 A m^{-2}, respectively.[20,21] The device based on a substituted poly(*p*-phenylene) emits light peaking at 424 nm, but the emission begins at 20 V with a luminance of 50 cd m^{-2} at 35 V.[22] Very recently, a blue-violet-emitting organic EL device using 4,4′-(*N*-carbazolyl)biphenyl (CBP) as an emitter, copper phthalocyanine as a hole transporter, and 2-(4-biphen-

* To whom correspondence should be addressed. Tel: +81-6-6879-7364. Fax: +81-6-6879-7367. e-mail: shirota@ap.chem.eng.osaka-u.ac.jp.

(1) Adachi, C.; Tsutsui, T.; Saito, S. *Appl. Phys. Lett*. **1990**, *56*, 799.
(2) Ohmori, Y.; Uchida, M.; Muro, K.; Yoshino, K. *Jpn. J. Appl. Phys*. **1991**, *30*, L1941.
(3) Grem, G.; Leditzky, G.; Ullrich, B.; Leising, G. *Adv. Mater*. **1992**, *4*, 36.
(4) Hamada, Y.; Adachi, C.; Tsutsui, T.; Saito, S. *Jpn. J. Appl. Phys*. **1992**, *31*, 1812.
(5) Hosokawa, C.; Higashi, H.; Nakamura, H.; Kusumoto, T. *Appl. Phys. Lett*. **1995**, *67*, 3853.
(6) Kido, J.; Kimura, M.; Nagai, K. *Chem. Lett*. **1996**, 47.
(7) Yang, Y.; Pei, Q.; Heeger, A. J. *J. Appl. Phys*. **1996**, *79*, 934.
(8) Salbeck, J.; Yu, N.; Bauer, J.; Weissörtel, F.; Bestgen, H. *Synth. Met*. **1997**, *91*, 209.
(9) Ogawa, H.; Ohnishi, K.; Shirota, Y. *Synth. Met*. **1997**, *91*, 243.
(10) Garten, F.; Hilberer, A.; Cacialli, F.; Esselink, F. J.; van Dam, Y.; Sclatmann, A. R.; Friend, R. H.; Klapwijk, T. M.; Hadziioannou, G. *Synth. Met*. **1997**, *85*, 1253.
(11) Noda, T.; Ogawa, H.; Shirota, Y. *Adv. Mater*. **1999**, *11*, 283.
(12) Kijima, Y.; Asai, N.; Tamura, S. *Jpn. J. Appl. Phys*. **1999**, *38*, 5274.
(13) Jiang, X.; Liu, S.; Ma, H.; Jen, A. K.-Y. *Appl. Phys. Lett*. **2000**, *76*, 1813.
(14) Noda, T.; Shirota, Y. *J. Lumin*. **2000**, *87*−*89*, 1168.
(15) Tang, B. Z.; Zhan, X.; Yu, G.; Lee, P. P. S.; Liu, Y.; Zhu, D. *J. Mater. Chem*. **2001**, *11*, 2974.
(16) Chan, L.-H.; Yeh, H.-C.; Chen, C.-T. *Adv. Mater*. **2001**, *13*, 1637.
(17) Wu, C. C.; Lin, Y. T.; Chiang, H. H.; Cho, T. Y.; Chen, C. W.; Wong, K. T.; Liao, Y. L.; Lee, G. H.; Peng, S. M. *Appl. Phys. Lett*. **2002**, *81*, 577.
(18) Kinoshita, M.; Shirota, Y. *Chem. Lett*. **2001**, 614.
(19) Hoshino, S.; Ebata, K.; Furukawa, K. *J. Appl. Phys*. **2000**, *87*, 1968.
(20) Kido, J.; Hongawa, K.; Okuyama, K.; Nagai, K. *Appl. Phys. Lett*. **1993**, *63*, 2627.
(21) Romero, D. B.; Nüesh, F.; Benazzi, T.; Adés, D.; Siove, A.; Zuppiroli, L. *Adv. Mater*. **1997**, *9*, 1158.
(22) Huang, J.; Zhang, H.; Tian, W.; Hou, J.; Ma, Y.; Shen, J.; Liu, S. *Synth. Met*. **1997**, *87*, 105.

10.1021/cm020849+ CCC: $25.00 © 2003 American Chemical Society
Published on Web 01/15/2003

ylyl)-5-(4-*tert*-butylphenyl)-1,3,4-oxadiazole as an electron transporter has been reported to emit light with an emission peak at ca. 390 nm, exhibiting a turn-on voltage of ca. 6.0 V, and having an external quantum efficiency of 1.25%.[23]

Amorphous molecular materials that form uniform amorphous thin films by themselves have demonstrated their suitability and versatility as materials for use in organic EL devices.[24−26] Good candidates for violet- to blue-violet-emitting materials can be found among amorphous molecular materials with hole-transporting properties, e.g., *N*,*N*′-bis(3-methylphenyl)-*N*,*N*′-diphenyl[1,1′-biphenyl]-4,4′-diamine (TPD).[1,27] The use of such materials as blue-violet emitters instead of hole transporters, however, requires either an electron transporter with an effective hole-blocking ability or a hole blocker inserted between the emitting and electron-transport layers. There have been reported a few electron transporters that function as effective hole blockers; a well-known electron transporter such as tris(8-quinolinolato)-aluminum (Alq_3) does not necessarily function well as an effective hole blocker for emitters with hole-transporting properties.[18] There is a previous report on a device using TPD as an emitter and 3-(4-biphenylyl)-4-phenyl-5-(4-*tert*-butylphenyl)-1,2,4-triazole (TAZ) as an electron transporter; however, the emission from TPD is accompanied by another, stronger one peaking at ca. 460 nm,[28] which may be attributable to the emission of exciplex formed between TPD and TAZ. The use of a hole blocker inserted between the emitting layer and the electron-transport layer in organic EL devices is a promising approach. In this device, the hole-blocking layer and the electron-transport layer play each role of confining holes within the emitting layer and facilitating electron injection from the cathode, respectively. It has been reported that bathocuproine serves as a hole blocker in organic EL devices;[12] however, its morphological and thermal stability are poor. In addition, it tends to form exciplexes with hole-transporting materials such as TPD, a stronger exciplex emission accompanying the blue-violet emission from TPD in the longer wavelength region from 440 to 600 nm.

It is a subject of current importance to develop new hole-blocking materials for use in organic EL devices. Such hole blockers are expected to enable the fabrication of not only blue-violet-emitting organic EL devices using emitters with hole-transporting properties, but also phosphorescent EL devices by utilizing excitation energy transfer from blue-violet emitters as the host materials to phosphorescent dopants. Hole-blocking materials for use in organic EL devices should fulfill several requirements. They should possess proper energy levels of the highest occupied molecular orbital (HOMO) and the lowest unoccupied molecular orbital (LUMO) to be able to block holes from escaping from the emitting layer into the electron-transport layer but to pass on electrons from the electron-transport layer to the emitting layer. In other words, the difference in the HOMO energy levels between the emitting material and the hole-blocking material should be much larger than that in their LUMO energy levels. They should not form any exciplexes with emitting materials having hole-transporting properties. In addition, they should form thermally and morphologically stable, uniform, amorphous thin films.

We report here the synthesis and properties of a new class of hole-blocking amorphous molecular materials, 1,3,5-tri(4-biphenylyl)benzene (TBB), 1,3,5-tris(4-fluorobiphenyl-4′-yl)benzene (F-TBB), 1,3,5-tris(9,9-dimethylfluoren-2-yl)benzene (TFB), and 1,3,5-tris[4-(9,9-dimethylfluoren-2-yl)phenyl]benzene (TFPB), and their application in blue-violet-emitting fluorescent and green-emitting phosphorescent organic EL devices using these materials as hole blockers. Amorphous molecular materials with hole-transporting properties, TPD, *N*,*N*′-bis(4-biphenylyl)-*N*,*N*′-diphenyl[1,1′-biphenyl]-4,4′-diamine (*p*-BPD),[29] and *N*,*N*′-bis[9,9-dimethylfluoren-2-yl]-*N*,*N*′-diphenyl-9,9-dimethylfluorene-2,7-diamine (PFFA),[30] together with a new amorphous molecular material, *N*,*N*-bis(9,9-dimethylfluorene-2-yl)aniline (F_2-PA), were used as blue-violet-emitting materials. A part of the present work has been previously reported as a communication.[31]

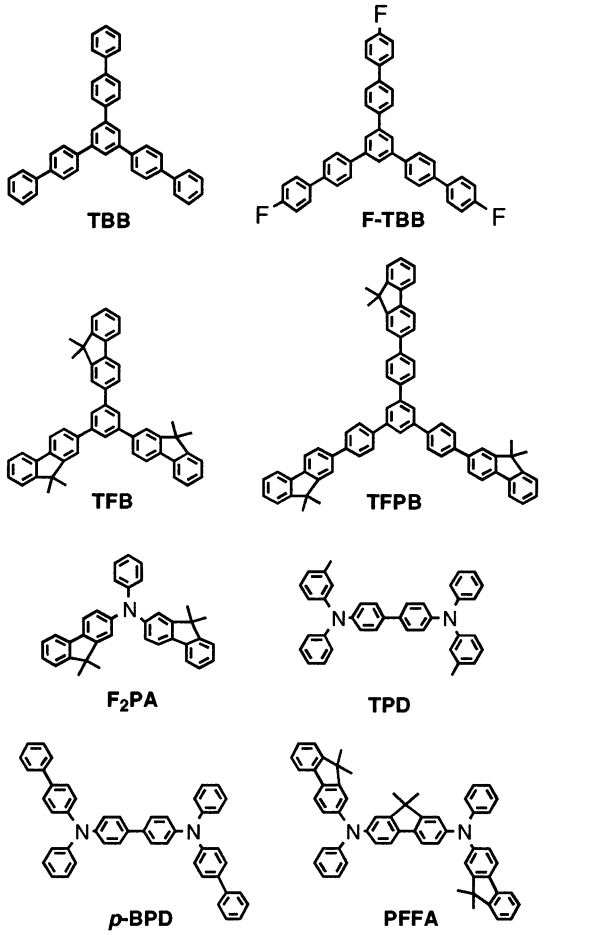

(23) Zou, L.; Savvate'ev, V.; Booher, J.; Kim, C.-H.; Shinar, J. *Appl. Phys. Lett*. **2001**, *79*, 2282.
(24) Shirota, Y. *J. Mater. Chem*. **2000**, *10*, 1.
(25) Mitschke, U.; Bäuerle, P. *J. Mater. Chem*. **2000**, *10*, 1471.
(26) Robinson, M. R.; Wang, S.; Heeger, A. J.; Bazan, G. C. *Adv. Funct. Mater*. **2001**, *11*, 413.
(27) Stolka, M.; Yanus, J. F.; Pai, D. M. *J. Phys. Chem*. **1984**, *88*, 4707.
(28) Kido, J.; Ohtaki, C.; Hongawa, K.; Okuyama, K.; Nagai, K. *Jpn. J. Appl. Phys*. **1993**, *32*, L917.
(29) Shirota, Y.; Okumoto, K.; Inada, Y. *Synth. Met*. **2000**, *111*−*112*, 387.

Experimental Section

Chemicals. 4-Acetylbiphenyl, 1,3,5-tribromobenzene, 1,3,5-triphenylbenzene, fluorene, 4-fluorophenylboronic acid, *N*,*N*-diphenylbenzidine, and aniline were obtained commercially. TPD and Alq_3 were obtained from Tokyo Chemical Industry Co. Ltd. and Shin-nittetsu Kagaku Co. Ltd., respectively. Gel permeation chromatography was performed by using an LC-908 recycling preparative HPLC (Japan Analytical Industry Co., Ltd.) with two columns for the separation of low-molecular-weight organic compounds: JAIGEL-1H and JAIGEL-2H (styrene polymer gels).

Synthesis of 2-Iodofluorene. 2-Iodofluorene was synthesized by the iodination of fluorene (100 g, 602 mmol) with iodine (80 g, 320 mmol) in the presence of ortho-periodinic acid (H_5IO_6) (20 g, 88 mmol) in 80% acetic acid aqueous solution at 80 °C for 4 h under nitrogen atmosphere. After the solution cooled, the solvent was removed by decantation and a brown solid was obtained. This was dissolved in toluene and washed with 5% $NaHSO_3$ aqueous solution to remove the remaining iodine. Then, the resulting solid was purified by alumina column chromatography using toluene as an eluent, followed by recrystallization from toluene. Yield: 105 g (60%), mp 131 °C.

Synthesis of 9,9-Dimethyl-2-iodofluorene. 2-Iodofluorene (60 g, 205 mmol) was dissolved in tetrahydrofuran (THF) and treated with potassium *tert*-butoxide (24 g, 214 mmol) to give a red solution, followed by methylation with methyliodide (30.4 g, 214 mmol). This procedure was repeated once more to yield 9,9-dimethyl-2-iodofluorene. This was purified by silica gel column chromatography using hexane as an eluent, followed by vacuum distillation. Yield: 49.2 g (75%), mp 63 °C.

Synthesis of 2,7-Diiodofluorene. 2,7-Diiodofluorene was synthesized by the iodination of fluorene (10 g, 60 mmol) with iodine (16 g, 64 mmol) in the presence of ortho-periodinic acid (H_5IO_6) (4.0 g, 17.6 mmol) in 80% acetic acid aqueous solution at 80 °C for 6 h under nitrogen atmosphere. After the solution cooled, the solvent was removed by decantation and a brown solid was obtained. This was dissolved in toluene and washed with 5% $NaHSO_3$ aqueous solution to remove the remaining iodine. Then, the resulting solid was purified by alumina column chromatography using toluene as an eluent, followed by recrystallization from toluene solution. Yield: 18.5 g (74%).

Synthesis of 9,9-Dimethyl-2,7-diiodofluorene. 2-Iodofluorene (10 g, 24 mmol) was dissolved in THF and treated with potassium *tert*-butoxide (3.0 g, 27 mmol) to give a red solution, followed by methylation with methyliodide (3.8 g, 27 mmol). This procedure was repeated once more to yield 9,9-dimethyl-2-iodofluorene. This was purified by silica gel column chromatography using toluene/hexane as an eluent. Yield: 8.0 g (75%), mp 198 °C.

Synthesis of *N*-(9,9-Dimethylfluoren-2-yl)aniline. *N*-(9,9-Dimethylfluoren-2-yl)aniline was synthesized by the Ullmann reaction of 9,9-dimethyl-2-iodofluorene (30 g, 94 mmol) with aniline (80 g, 860 mmol) at 170 °C for 8 h in the presence of copper powder (12 g), potassium carbonate (20 g), and 18-crown-6-ether (2.0 g) and purified by silica gel column chromatography using toluene/hexane as an eluent, followed by recrystallization from toluene/hexane. Yield: 16.9 g (63%), mp 101 °C.

Synthesis of 1,3,5-Tris(4-iodophenyl)benzene. 1,3,5-Tris(4-iodophenyl)benzene was synthesized by the iodination of 1,3,5-triphenylbenzene (15 g, 49 mmol) with iodine (60 g, 237 mmol) in the presence of ortho-periodinic acid (H_5IO_6) (20 g, 88 mmol) in 80% acetic acid aqueous solution at 80 °C for 6 h under nitrogen atmosphere. After the solution cooled, the solvent was removed by decantation and a brown solid was obtained. This was dissolved in toluene and washed with 5% $NaHSO_3$ aqueous solution to remove the remaining iodine. Then, the resulting solid was purified by alumina column chromatography using toluene as an eluent, followed by recrystallization from toluene solution. Yield: 17.4 g (52%), mp 258 °C.

Synthesis of F_2PA. F_2PA was synthesized by the Ullmann reaction of 9,9-dimethyl-2-iodofluorene (50 g, 156 mmol) with aniline (5.5 g, 59 mmol) in mesitylene at 170 °C for 8 h in the presence of copper powder (7.5 g), potassium carbonate (35 g), and 18-crown-6-ether (1.5 g) and purified by silica gel column chromatography using toluene/hexane as an eluent, followed by recrystallization from toluene/hexane. Yield: 20 g (71%). This was further purified by column chromatography and recrystallization, to obtain highly pure sample, mp 196 °C.

F_2PA. MS: *m*/*e* 477(M^+). EA: Found C, 90.38; H, 6.55; N, 2.93% Calcd for $C_{36}H_{21}N$, C, 90.53; H, 6.54, N, 2.93%. ^{1}H NMR (THF-d_8): δ (ppm) 7.74 (2H, d), 7.72 (2H, d), 7.49 (2H, d), 7.35−7.30 (6H,m), 7.27 (2H, t), 7.17 (2H, d), 7.07 (1H, t), 7.04 (2H,d), 1.41 (12H, s).

Synthesis of *p*-BPD. *p*-BPD was synthesized by the Ullmann reaction of 4-iodobiphenyl (12.5 g, 45 mmol) with *N*,*N*-diphenylbenzidine (5.0 g, 15 mmol) in mesitylene at 170 °C for 8 h in the presence of copper powder (3.6 g), potassium carbonate (15 g), and 18-crown-6-ether (0.8 g) and purified by silica gel column chromatography using toluene/hexane as an eluent, followed by recrystallization from toluene/hexane. Yield: 4.7 g (49%). This was further purified by column chromatography and recrystallization, to obtain highly pure sample, mp 213 °C.

p-BPD. MS: *m*/*e* 640(M^+). EA: Found C, 89.73; H, 5.76; N, 4.27%. Calcd for $C_{48}H_{36}N_2$, C, 89.97; H, 5.66; N, 4.37%. ^{1}H NMR (THF-d_8): δ (ppm) 7.02 (2H, t), 7.12−7.16 (12H, m), 7.24−7.28 (6H, m), 7.37 (4H, t), 7.53 (8H, t), 7.59 (4H, d).

Synthesis of PFFA. PFFA was synthesized by the Ullmann reaction of 2,7-diiodofluorene (10.0 g, 5.2 mmol) with *N*-(9,9-dimethylfluoren-2-yl)aniline (6.0 g, 21 mmol) in mesitylene at 170 °C for 8 h in the presence of copper powder (3.0 g), potassium carbonate (10 g), and 18-crown-6 ether (0.7 g) and purified by silica gel column chromatography using toluene/hexane as an eluent, followed by recrystallization from toluene/hexane. Yield: 1.8 g (47%). This was further purified by column chromatography and recrystallization, to obtain highly pure sample, mp 263 °C.

PFFA. MS: *m*/*e* 760 (M^+). EA: Found C, 89.86; H, 6.55; N, 3.58%. Calcd for $C_{57}H_{48}N_2$, C, 89.96; H, 6.38; N, 3.68%. ^{1}H NMR (THF-d_8): δ (ppm) 7.64 (2H, d), 7.61 (2H, d), 7.55 (2H, d), 7.38 (2H, t), 7.26−7.23 (10H, m), 7.19 (2H, t), 7.15 (4H, t), 7.03 (4H, t), 6.99 (2H, t), 1.39 (12H, s), 1.34 (6H, s).

Synthesis of TBB. TBB was prepared by the condensation reaction of 4-acetylbiphenyl (25 g, 127 mmol) in the presence of trifluoromethanesulfuric acid (5 mL) in toluene at 110 °C for 8 h, and purified by silica gel column chromatography using toluene as an eluent and recrystallization from toluene. Yield 14 g (63%). This was further purified by sublimation repeatedly, to obtain highly pure sample, mp 233 °C.

TBB. MS: *m*/*e* 534(M^+). EA: Found C, 94.28; H, 5.58%. Calcd for $C_{42}H_{30}$, C, 94.34; H, 5.66%. ^{1}H NMR ($CDCl_3$-d_8): δ (ppm) 7.89 (3H, s), 7.82 (6H, d), 7.81 (6H, t), 7.74 (6H, d), 7.69 (3H, t), 7.68 (6H, d).

Synthesis of F-TBB. F-TBB was synthesized by the Suzuki coupling reaction of 1,3,5-tris(4-iodophenyl)benzene (2.5 g, 3.7 mmol) with 4-fluorophenylboronic acid (5.0 g, 35 mmol) in THF/2 N K_2CO_3 aqueous solution at 70 °C for 8 h in the presence of tetrakis(triphenylphosphine)palladium(0) (0.5 g, 0.4 mmol), and purified by silica gel column chromatography using toluene/hexane as an eluent and recrystallization from toluene/hexane. Yield: 1.5 g (70%). This was further purified by column chromatography, gel permentation chromatography, and recrystallization, to obtain highly pure sample, mp 236 °C.

F-TBB. MS: *m*/*e* 588(M^+). EA: Found C, 85.68; H, 4.60%. Calcd for $C_{42}H_{37}F_3$, C, 85.69; H, 4.62%. ^{1}H NMR ($CDCl_3$-d_8): δ (ppm) 7.88 (3H, s), 7.81 (6H, d), 7.68 (6H, d), 7.63 (6H, dd), 7.17 (6H, t).

Synthesis of TFB. TFB was synthesized by the Suzuki coupling reaction of 1,3,5-tribromobenzene (4.8 g, 7.7 mmol) with 9,9-dimethylfluoren-2-ylboronic acid (11 g, 46 mmol) in THF/2 N K_2CO_3 aqueous solution at 70 °C for 8 h in the presence of tetrakis(triphenylphosphine)palladium(0) (0.5 g,

(30) Okumoto, K.; Shirota, Y. *Mater. Sci. Eng. B* **2001**, *85*, 135.
(31) Okumoto, K.; Shirota, Y. *Appl. Phys. Lett.* **2001**, *79*, 1231.

0.4 mmol), and purified by silica gel column chromatography using toluene/hexane as an eluent and recrystallization from toluene/hexane. Yield: 2.6 g (52%). This was further purified by column chromatography, gel permentation chromatography, and recrystallization, to obtain highly pure sample, mp 342 °C.

TFB. MS: *m*/*e* 654(M^+). EA: Found C, 93.25; H, 6.56%. Calcd for $C_{51}H_{42}$, C, 93.54; H,6.46%. ^{1}H NMR ($CDCl_3$-d_8): δ (ppm) 7.88 (3H, s), 7.84 (3H, d), 7.77 (3H, d), 7.77 (3H, s), 7.72 (3H, d), 7.46 (3H, d), 7.36 (3H, t), 7.33 (3H, t), 1.57 (18H, s).

Synthesis of TFPB. TFPB was synthesized by the Suzuki coupling reaction of 1,3,5-tris(iodophenyl)benzene (5.2 g, 7.7 mmol) with 9,9-dimethylfluoren-2-ylboronic acid (11 g, 46 mmol) in THF/2 N K_2CO_3 aqueous solution at 70 °C for 8 h in the presence of tetrakis(triphenylphosphine)palladium(0) (0.5 g, 0.4 mmol), and purified by silica gel column chromatography using toluene/hexane as eluent and recrystallization from toluene/hexane. Yield 1.8 g (27%). This was further purified by column chromatography, gel permentation chromatography, and recrystallization, to obtain highly pure sample, mp 264 °C.

TFPB. MS: *m*/*e* 882(M^+). EA: Found C, 93.63; H, 6.29; Calcd for $C_{69}H_{54}$, C, 93.84; H, 6.16%. ^{1}H NMR ($CDCl_3$): δ (ppm) 7.93 (3H, s), 7.86 (6H, d), 7.84−7.81 (9H, m), 7.78 (3H, d), 7.77 (3H, s), 7.67 (3H, s), 7.47 (3H, d), 7.37 (3H,t), 7.34 (3H, t), 1.57 (18H, s).

Measurements. Cyclic voltammetry was carried out for 1.0 $\times$ 10^{-3} mol dm^{-3} dichloromethane solution of each compound containing 0.1 mol dm^{-3} tetra-*n*-butylammonium perchlorate (0.1 mol dm^{-3}) as supporting electrolyte. A platinum disk (1.6 mm diam.), platinum wire, and Ag/$AgNO_3$ (0.01 mol dm^{-2} in acetonitrile) were used as working, counter, and reference electrodes, respectively. Scan rate was 100 mV s^{-1}. Electronic absorption and photoluminescence (PL) spectra were measured with a HITACHI U-3500 spectrophotometer and a HITACHI model F-4500 fluorescence spectrophotometer, respectively. Fluorescence quantum efficiency was determined with reference to sulfuric acid aqueous solution of quinine sulfate.

Fabrication of Organic EL Devices. Organic EL devices were fabricated by successive vacuum deposition of the organic materials onto an ITO-coated glass substrate at a deposition rate of 0.2−0.3 nm s^{-1} at 10^{-5} Torr. Then, an alloy of magnesium and silver (ca 10:1 volume ratio) was deposited onto the organic layer by simultaneous evaporation from two separate sources. Thin films of the organic materials for the measurement of PL spectra were vacuum deposited onto a transparent glass substrate. The current versus voltage and the current versus luminance characteristics were measured with an Advantest TR6143 electrometer and a photoluminance meter Minolta LS-100. EL spectra were measured with a Hitachi model F-4500 fluorescence spectrophotometer.

Results and Discussion

Synthesis and Properties of Blue-Violet-Emitting Amorphous Molecular Materials, F_2PA, *p*-BPD, and PFFA. The compounds F_2PA, *p*-BPD, and PFFA were synthesized by using the Ullmann coupling reactions as shown in Scheme 1.

These compounds with electron-donating properties undergo reversible anodic oxidation. Figure 1 shows the cyclic voltammograms of F_2PA and PFFA. Whereas *p*-BPD and PFFA exhibit two sequential anodic and the corresponding cathodic waves in their cyclic voltammograms, F_2PA shows one anodic and the corresponding cathodic waves. All these compounds were found to exhibit blue-violet fluorescence with relatively high quantum efficiencies ranging from 0.56 to 0.78 in solution. They readily form amorphous glasses with well-defined glass-transition temperatures (T_gs). Therefore, they are expected to serve as blue-violet emitters in the presence of both the hole blocker and electron transporter in organic EL devices. The T_gs, half-wave

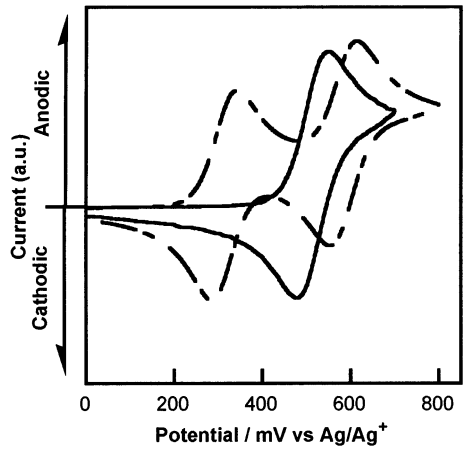

Figure 1. Cyclic voltammograms of F_2PA (solid line) and PFFA (partially dotted line).

Scheme 1. Synthetic Routes of F_2PA, *p*-BPD, and PFFA

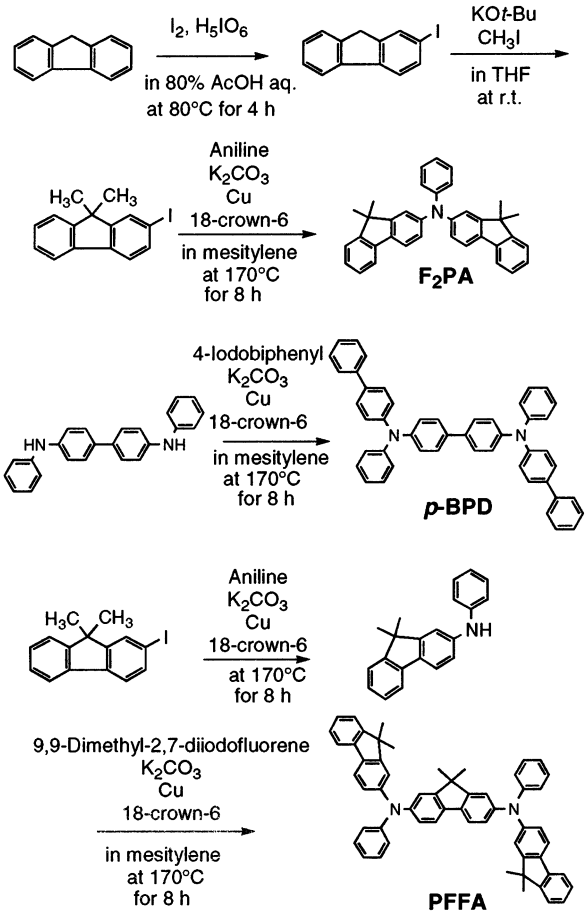

oxidation potentials ($E^{ox}_{1/2}$), electronic absorption and fluorescence band maxima (λ^{abs}_{max} and λ^{fl}_{max}), fluorescence quantum efficiencies (Φ_{fl}), and HOMO−LUMO energy gaps of F_2PA, *p*-BPD, and PFFA together with those of TPD are summarized in Table 1.

Synthesis, Properties, and Morphology of Hole-Blocking Amorphous Molecular Materials TBB, F-TBB, TFB, and TFPB. The molecular design of a new class of hole blockers, TBB, F-TBB, TFB, and TFPB, is based on the consideration that the molecules should have rather high oxidation potentials and large HOMO−LUMO energy gaps. They were synthesized by

Table 1. Glass-Transition Temperatures (T_gs), Half-Wave Oxidation Potentials ($E^{ox}_{1/2}$), Electronic Absorption and Fluorescence Band Maxima (λ^{abs}_{max} and λ^{fl}_{max}), Fluorescence Quantum Efficiencies (Φ_{fl}), and HOMO−LUMO Energy Gaps for F_2PA, *p*-BPD, PFFA, and TPD

	T_g (°C)[a]	$E^{ox}_{1/2}$ (V vs Ag/Ag$^+$ (0.01 mol dm^{-3}))[b]	λ^{abs}_{max} (nm)[c], log ϵ	λ^{fl}_{max} (nm)[d]	Φ_{fl}	HOMO−LUMO energy gap (eV)[e]
F_2PA	82	0.51	368 (4.58)	400	0.56	3.17
p-BPD	102	0.50	358 (4.76)	406	0.78	3.16
PFFA	135	0.32	392 (4.80)	414	0.76	3.03
TPD	63	0.48	352 (4.64)	399	0.68	3.19

[a] Determined by DSC. [b] Determined by cyclic voltammetry in dichloromethane solution. Scan rate: 100 mV s^{-1}. [c] Measured in THF solution. [d] Determined with reference to sulfuric acid aqueous solution of quinine sulfate. [e] Estimated from the edge of the electronic absorption band.

Scheme 2. Synthetic Routes of TBB, F-TBB, TFB, and TFPB

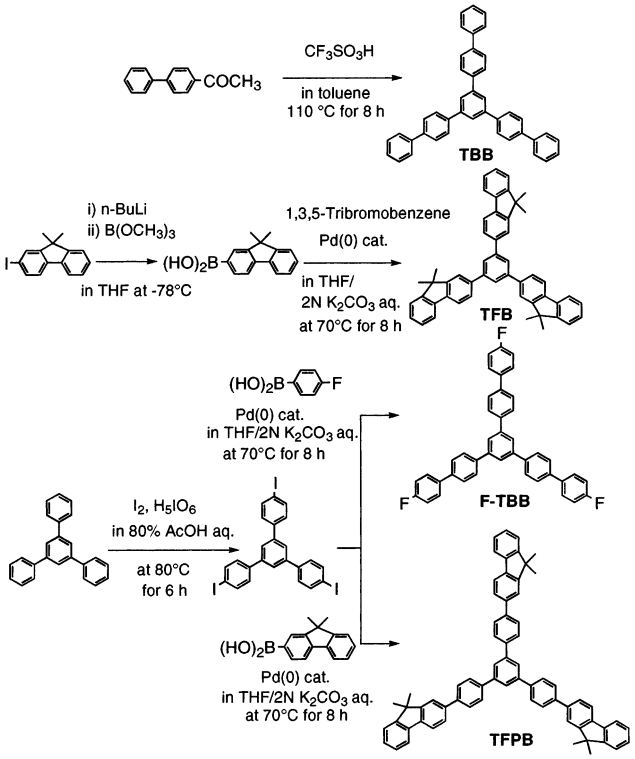

the condensation reaction or the Suzuki coupling reaction. Scheme 2 shows the synthetic routes of these hole blockers.

Although F-TBB and TFPB underwent reversible anodic oxidation, the anodic oxidation processes of TBB and TFB were irreversible. The irreversibility of anodic oxidation does not prevent them from the role of the hole blocker, because they serve to pass on electrons from the electron-transport layer to the emitting layer. The cathodic reduction of all the compounds was not observed in the potential region down to −2.3 V vs Ag/Ag$^+$ (0.01 mol dm^{-3}) reference electrode due to their weaker electron-accepting properties relative to that of Alq_3. The oxidation potentials of these compounds are much higher than those of the blue-violet emitting materials, F_2PA, TPD, *p*-BPD, and PFFA. It is noteworthy that all these compounds do not form any exciplexes with the above emitters with hole-transporting properties. In addition, the absorption band edges of the materials are in the wavelength shorter than 360 nm, indicating that they have large HOMO−LUMO energy gaps.

These compounds were found to form stable amorphous glasses with well-defined T_gs, as evidenced by differential scanning calorimetry (DSC), powder X-ray diffraction, and polarizing microscopy. The polycrystalline sample of TFB obtained by recrystallization from toluene/hexane mixed solution melted at 342 °C to give an isotropic liquid. When this isotropic liquid was cooled on standing in air, it formed an amorphous glass without any crystallization. When the glass sample was again heated, glass transition was observed at 133 °C to give a supercooled liquid. Upon further heating above the T_g, crystallization took place at ca. 175 °C to give the same crystal as that obtained from recrystallization. The incorporation of a rigid fluorene moiety leads to higher T_gs. This has been shown for other classes of amorphous molecular materials.[30,32,33] Table 2 summarizes the T_gs, oxidation potentials ($E^{ox}_{1/2}$ or $E^{ox}_{p/2}$), electronic absorption band maxima, and HOMO−LUMO energy gaps of TBB, F-TBB, TFB, and TFPB determined from the edge of the electronic absorption bands. Thus, all the synthesized compounds meet the requirements for the hole blocker for use in organic EL devices.

It should be noted that among the synthesized hole-blocking materials, TBB, F-TBB, and TFPB exhibit polymorphism in addition to forming amorphous glasses. That is, the polycrystalline sample of TBB (crystal A) obtained by recrystallization from benzene melted at 233 °C to give an isotropic liquid. When the isotropic liquid was cooled on standing in air, it formed an amorphous glass without any crystallization. When the glass sample was again heated, glass-transition phenomenon was observed at 88 °C to give a supercooled liquid. Upon further heating above the T_g, crystallization took place at ca. 120 °C to give another crystal (crystal B), which melted at 215 °C. Upon further heating, no crystallization took place. F-TBB also exhibited similar morphological changes. Figure 2 shows the DSC curves of F-TBB. The polycrystalline sample of F-TBB (crystal A) obtained by recrystallization from toluene/hexane mixed solution melted at 236 °C to give an isotropic liquid. When this isotropic liquid was cooled on standing in air, it formed an amorphous glass. When the glass sample was again heated, glass-transition phenomenon was observed at 87 °C to give a supercooled liquid. Upon further heating above the T_g, crystallization took place at ca. 130 °C to give another crystal (crystal B), which melted at 165 °C. When this isotropic liquid was cooled, the amorphous glass was formed, and the same DSC trace was observed repeatedly. TFPB was found to take up four different crystal structures. The

(32) Shirota, Y.; Kinoshita, M.; Noda, T.; Okumoto, K.; Ohara, T. *J. Am. Chem. Soc.* **2000**, *122*, 11021.
(33) Okumoto, K.; Shirota, Y. *Chem. Lett.* **2001**, 1034.

Table 2. Glass-Transition Temperatures (T_gs), Oxidation Potentials ($E^{ox}_{1/2}$ or $E^{ox}_{p/2}$), Electronic Absorption Band Maxima (λ^{abs}_{max}) and Molar Extinction Coefficient (ϵ) in THF Solution, and HOMO−LUMO Energy Gaps of TBB, F-TBB, and TFB

	T_g (°C)[a]	$E^{ox}_{1/2}$ or $E^{ox}_{p/2}$ (V vs Ag/Ag^+ (0.01 mol dm^{-3}))[b]	λ^{abs}_{max} (nm)[c], log ϵ	HOMO−LUMO energy gap (eV)[d]
TBB	88	1.32	289 (5.00)	3.84
F-TBB	87	1.29	288 (5.04)	3.85
TFB	133	1.25	317 (5.07)	3.69
TFPB	149	1.12	324 (5.20)	3.49

[a] Determined by DSC. [b] Determined by cyclic voltammetry in dichloromethane solution. Scan rate: 100 mV s^{-1}. [c] Measured in THF solution. [d] Determined from their absorption band edges.

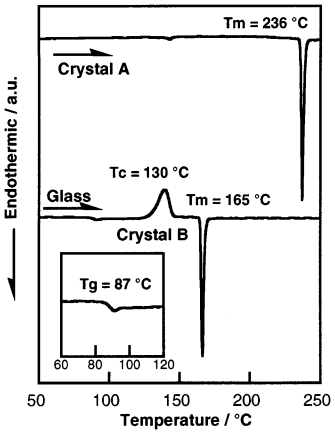

Figure 2. DSC curves of F-TBB. Heating rate: 5 °C min^{-1}.

polycrystalline sample of TFPB (crystal A) obtained by recrystallization from toluene/hexane solution melted at 235 °C, instantly followed by crystallization at ca. 240 °C to form another crystal (crystal B). On further heating, crystal B underwent solid−solid-phase transition at 255 °C to form another crystal (crystal C). Crystal C also underwent solid−solid-phase transition at 258 °C to form another crystal (crystal D), which melted at 263 °C to form isotropic liquid. The resulting isotropic liquid formed an amorphous glass via a supercooled liquid on cooling in air. When the glass sample was again heated, glass-transition phenomenon was observed at 149 °C. On further heating, crystallization took place at ca. 205 °C to give crystal B, and hereafter the same DSC curve as described above was obtained repeatedly. The phenomena of polymorphism suggest the existence of different conformers, which is responsible for the ease of amorphous glass formation. Such polymorphism has been observed for a number of amorphous molecular materials.[24,34−36]

Fabrication and Performance of Blue-Violet-Emitting Organic EL Devices. A new class of hole-blocking amorphous molecular materials developed in the present study is expected to enable blue-violet emission from the emitting materials with hole-transporting properties in organic EL devices. The synthesized hole-blocking materials as well as the emitting materials form uniform amorphous films by vacuum deposition. Multilayer organic EL devices were fabricated using F_2PA, TPD, *p*-BPD, and PFFA as emitters, TBB, F-TBB, and TFPB as hole-blockers, 4,4′,4″-tris-[3-methylphenyl(phenyl)amino]triphenylamine (*m*-MTDATA)[37,38] as a hole transporter, and Alq_3 as an electron transporter. The fabricated devices consisted of four layers in the order of hole-transport layer (HTL), emitting layer (EML), hole-blocking layer (HBL), and electron-transport layer (ETL) sandwiched between the ITO and MgAg electrodes, as shown in Figure 3. The total thickness of the organic layers was fixed as 100 nm. The fabricated organic EL devices are the following: ITO/*m*-MTDATA (50 nm)/F_2PA (20 nm)/F-TBB (10 nm)/Alq_3 (20 nm)/MgAg (device A); ITO/*m*-MTDATA (50 nm)/F_2PA (20 nm)/F-TBB (20 nm)/Alq_3 (10 nm)/MgAg (device B); ITO/*m*-MTDATA (50 nm)/TPD (20 nm)/F-TBB (10 nm)/Alq_3 (20 nm)/MgAg (device C); ITO/*m*-MTDATA (50 nm)/*p*-BPD (20 nm)/F-TBB (10 nm)/Alq_3 (20 nm)/MgAg (device D); ITO/*m*-MTDATA (50 nm)/PFFA (20 nm)/F-TBB (10 nm)/Alq_3 (20 nm)/MgAg (device E); ITO/*m*-MTDATA (50 nm)/F_2PA (20 nm)/TBB (20 nm)/Alq_3 (10 nm)/MgAg (device F); and ITO/*m*-MTDATA (50 nm)/PFFA (20 nm)/TFPB (10 nm)/Alq_3 (20 nm)/MgAg (device G).

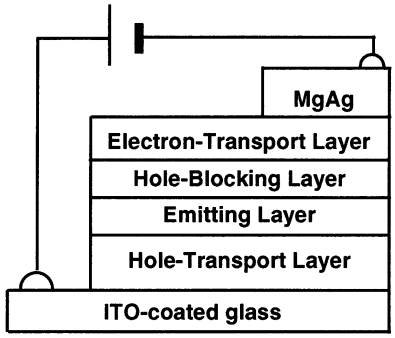

Figure 3. Side view of multilayer organic EL devices.

Blue-violet emissions peaking at 404, 405, 415, and 422 nm were observed for the devices using TPD, F_2-PA, *p*-BPD, and PFFA as emitters, respectively. Figure 4 shows the EL spectra of devices A and G and the PL spectra of the thin films of F_2PA and PFFA. The EL spectrum of each device was in good agreement with the PL spectrum of each emitting material. The results indicate that the EL of each device originates from the electronically excited singlet state of each emitter, generated by the recombination of injected holes and electrons, and that the hole carriers were blocked effectively from escaping from the emitting layer to the electron-transport layer in all the devices. Neither emission from Alq_3 nor any emission attributable to exciplexes between the emitting materials and the hole blockers was observed. No voltage dependence of the EL spectra was observed either. It should be noted that in

(34) Ishikawa, W.; Inada, H.; Nakano, H.; Shirota, Y. *Chem. Lett.* **1991**, 1731.
(35) Ishikawa, W.; Inada, H.; Nakano, H.; Shirota, Y. *J. Phys. D* **1993**, *26*, B94.
(36) Ueta, E.; Nakano, H.; Shirota, Y. *Chem. Lett.* **1994**, 2397.
(37) Shirota, Y.; Kobata, T.; Noma, N. *Chem. Lett.* **1989**, 1145.
(38) Shirota, Y.; Kuwabara, Y.; Inada, H.; Wakimoto, H.; Nakada, H.; Yonemoto, Y.; Kawami, S.; Imai, K. *Appl. Phys. Lett.* **1994**, *65*, 807.

Table 3. Performance of Organic EL Devices, ITO/*m*-MTDATA/Emitter/Hole Blocker/Alq_3/MgAg

device	emitter	hole blocker	EL peak wavelength (nm)	turn-on voltage[a] (V)	maximum luminance (cd m^{-2})	external quantum efficiency[b] (%)
A[c]	F_2PA	F-TBB	405	4.0	1600 (at 14.0 V)	1.75
B[d]	F_2PA	F-TBB	405	4.5	1820 (at 14.0 V)	1.95
C[c]	TPD	F-TBB	404	4.0	3960 (at 15.0 V)	1.40
D[c]	*p*-BPD	F-TBB	415	4.0	2550 (at 12.0 V)	1.25
E[c]	PFFA	F-TBB	422	3.0	3100 (at 12.0 V)	1.10
F[d]	F_2PA	TBB	405	5.0	2100 (at 15.0 V)	1.60
G[c]	PFFA	TFPB	422	3.0	2200 (at 13.0 V)	1.08

[a] Voltage to obtain a luminance greater than 0.1 cd m^{-2}. [b] At a luminance of 100 cd m^{-2}. [c] ITO/*m*-MTDATA (50 nm)/emitter (20 nm)/hole blocker (10 nm)/Alq_3 (20 nm)/MgAg. [d] ITO/*m*-MTDATA (50 nm)/emitter (20 nm)/hole blocker (20 nm)/Alq_3 (10 nm)/MgAg.

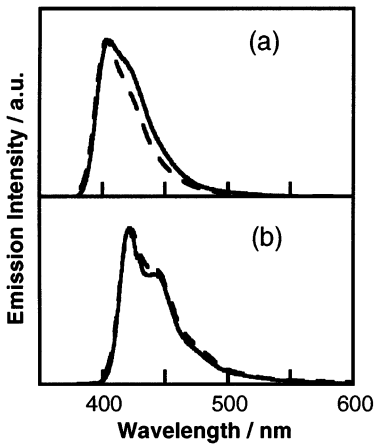

Figure 4. EL spectra of (a) device A and (b) device G at 6.0 V (solid line) and PL spectra of F_2PA (a) and PFFA (b) thin films (broken line). Device A: ITO/*m*-MTDATA (50 nm)/F_2PA (20 nm)/F-TBB (10 nm)/Alq_3 (20 nm)/MgAg. Device G: ITO/*m*-MTDATA (50 nm)/PFFA (20 nm)/TFPB (10 nm)/Alq_3 (20 nm)/MgAg.

the absence of the hole-blocking layer, green emission from Alq_3 took place.[29,30] Thus, the use of the present novel class of hole-blocking amorphous molecular materials enabled blue-violet emission from the emitters such as F_2PA, TPD, *p*-BPD, and PFFA in multilayer organic EL devices. The full width at the half-maximum of the EL spectra for all the devices were relatively narrow, being approximately 40 ± 2 nm. The CIE1931 chromaticity coordinates (x, y) of the emissions of devices A, C, D, and G using F_2PA, TPD, *p*-BPD, and PFFA as emitters were (0.160, 0.028), (0.163, 0.040), (0.161, 0.064), and (0.162, 0.056), respectively, as shown in Figure 5.

Figure 6 shows the luminance versus applied voltage and injected current density versus applied voltage characteristics for devices A, B, and G. Table 3 summarizes the EL peak wavelengths, turn-on voltages, maximum luminances, and external quantum efficiencies for each device. Each device exhibited high performance with low turn-on voltages from 3 to 5 V and relatively high external quantum efficiencies from 1.08 to 1.95%. The maximum luminance was also high, considering the low visibility of blue-violet light. The device B with the F-TBB hole-blocking layer of 20-nm thickness and the F_2PA emitting layer of 20-nm thickness exhibited the highest external quantum efficiency of 1.95% among the devices fabricated in the present study.

The high performance of the fabricated devices is attributed to both relatively high fluorescence quantum efficiencies of F_2PA, TPD, *p*-BPD, and PFFA, and the effective hole-blocking ability of TBB, F-TBB, and TFPB. Figure 7 shows the HOMO−LUMO energy levels (referenced to vacuum) of the materials (*m*-MTDATA, PFFA, TFPB, and Alq_3) used in device G. The values of *m*-MTDATA and Alq_3 were determined in our previous studies.[38] On the basis of the oxidation potential ($E^{ox}_{1/2}$ = 0.06 V vs Ag/Ag^+ 0.01 mol dm^{-3})[37] and the HOMO energy levels (5.1 eV)[38] of *m*-MTDATA, the HOMO energy levels of PFFA and TFPB were estimated from their oxidation potentials determined by cyclic voltammetry. Likewise, the LUMO energy levels of PPFA and TFPB were estimated from their electronic absorption edges and HOMO energy levels. The efficiency of TFPB in its function as the hole blocker is illustrated by the positions of its HOMO and LUMO energy levels relative to those of the neighboring PFFA and Alq_3 layers. While the TFPB LUMO level lies between those of PFFA and Alq_3, smoothly passing on the electrons coming from Alq_3 to the emitting layer, the HOMO level of TFPB lies well beneath that of Alq_3, effectively widening the gap significantly for holes trying to escape from the PFFA layer, thus blocking them and facilitating the blue-violet emission from PFFA. In the case of the other hole blockers, TBB, F-TBB, and TFB, the energy level difference between the hole-blocking materials and the emitting materials are larger than those for TFPB and the emitters, and hence, TBB, F-TBB, and TFB function as better hole blockers than TFPB.

Fabrication of Phosphorescent Organic EL Device. Organic EL devices utilizing phosphorescence emission have recently received a great deal of attention from the viewpoint of attaining higher quantum efficiency than that of the fluorescence-based organic EL devices.[39,40] Iridium complexes have been used as emissive dopants, and CBP, poly(*N*-vinylcarbazole), or 4,4′,4″-tri(*N*-carbazolyl)triphenylamine (TCTA)[41] that emit blue-violet light have been used as host materials.[42−45] A phosphorescent EL device using a green-emitting iridium complex doped in a TCTA host material and a starburst perfluorinated phenylene as a hole- and exciton-block layer has recently been reported to exhibit

(39) Baldo, M. A.; O'Brien, D. F.; You, Y.; Shoustikov, A.; Sibley, S.; Thompson, M. E.; Forrest, S. R. *Nature* **1998**, *395*, 151.
(40) Baldo, M. A.; Lamansky, S.; Burrows, P. E.; Thompson, M. E.; Forrest, S. R. *Appl. Phys. Lett.* **1999**, *75*, 4.
(41) Kuwabara, Y.; Ogawa, H.; Inada, H.; Noma, N.; Shirota, Y. *Adv. Mater.* **1994**, *6*, 677.
(42) Baldo, M. A.; Lamansky, S.; Burrows, P. E.; Thompson, M. E.; Forrest, S. R. *Appl. Phys. Lett.* **1999**, *75*, 4.
(43) Lee, C.-L.; Lee, K. B.; Kim, J.-J. *Appl. Phys. Lett.* **2000**, *77*, 2280.
(44) Lamansky, S.; Djurovich, P.; Murphy, D.; Abdel-Razzaq, F.; Lee, H.-E.; Adachi, C.; Burrows, P. E.; Forrest, S. R.; Thompson, M. E. *J. Am. Chem. Soc.* **2001**, *123*, 4304.
(45) Ikai, M.; Tokito, S.; Sakamoto, Y.; Suzuki, T.; Taga, Y. *Appl. Phys. Lett.* **2001**, *79*, 156.

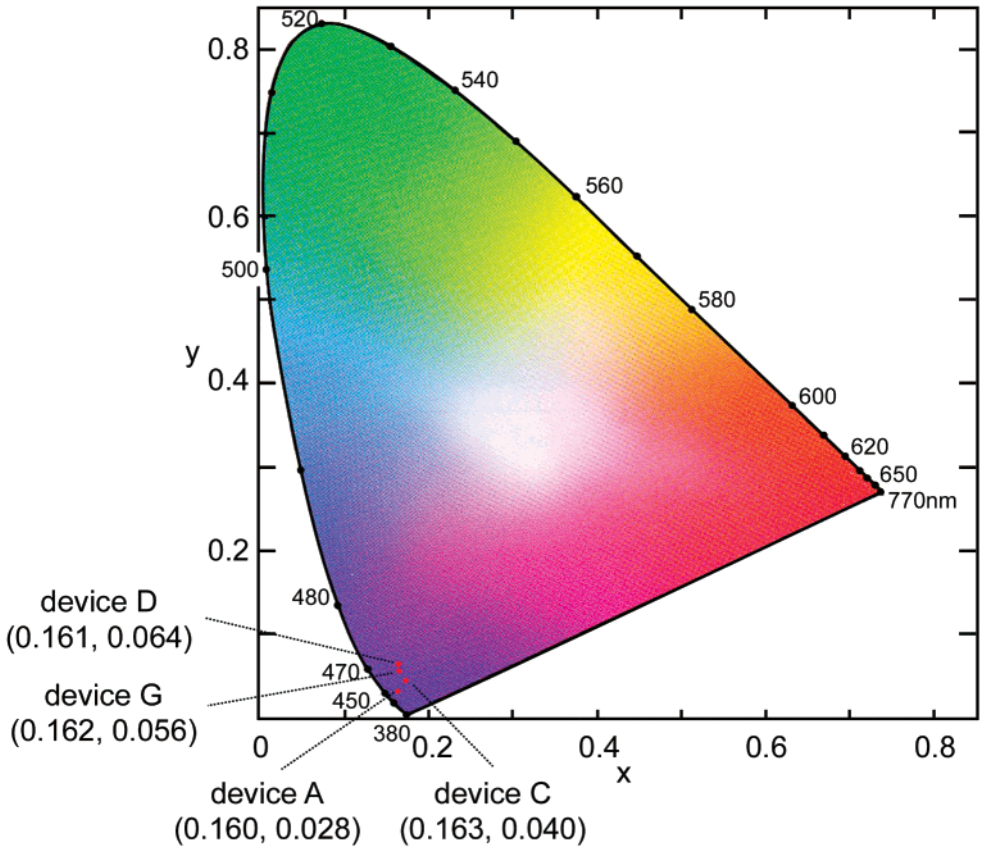

Figure 5. CIE1931 chromaticity coordinates (x, y) for devices A, C, D, and G. Device A: ITO/*m*-MTDATA (50 nm)/F_2PA (20 nm)/F-TBB (10 nm)/Alq_3 (20 nm)/MgAg. Device C: ITO/*m*-MTDATA (50 nm)/TPD (20 nm)/F-TBB (10 nm)/Alq_3 (20 nm)/MgAg. Device D: ITO/*m*-MTDATA (50 nm)/*p*-BPD (20 nm)/F-TBB (10 nm)/Alq_3 (20 nm)/MgAg. Device G: ITO/*m*-MTDATA (50 nm)/PFFA (20 nm)/TFPB (10 nm)/Alq_3 (20 nm)/MgAg.

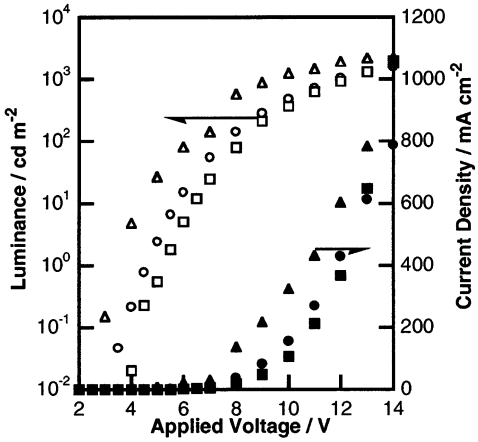

Figure 6. Luminance versus applied voltage characteristics for devices A (circle), B (square), and G (triangle), and current density versus applied voltage characteristics for devices A (filled circle), B (filled square), and G (filled triangle). Device A: ITO/*m*-MTDATA (50 nm)/F_2PA (20 nm)/F-TBB (10 nm)/Alq_3 (20 nm)/MgAg. Device B: ITO/*m*-MTDATA (50 nm)/F_2-PA (20 nm)/F-TBB (20 nm)/Alq_3 (10 nm)/MgAg. Device G: ITO/*m*-MTDATA (50 nm)/PFFA (20 nm)/TFPB (10 nm)/Alq_3 (20 nm)/MgAg.

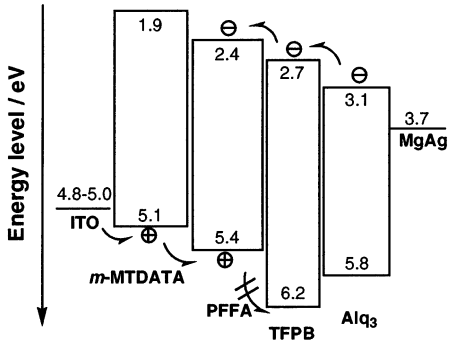

Figure 7. HOMO−LUMO energy levels (referenced to vacuum) of *m*-MTDATA, PFFA, TFPB, and Alq_3.

high performance.[45] The selection of host materials is of crucial importance for realizing efficient energy transfer from the host as the recombination center to the phosphorescent dopant. For effective singlet excitation energy transfer, the fluorescence band of the host material should well overlap with the absorption band of the dopant. The present blue-violet emitters are expected to act as host materials for the phosphorescent dopant. In the present study, F_2PA and tris(2-phenylpyridine)iridium ($Ir(ppy)_3$) were selected as the host and the phosphorescent dopant, respectively.

An organic EL device using F_2PA as the host material, $Ir(ppy)_3$ as a phosphorescence dopant, and F-TBB as the hole blocker, ITO/*m*-MTDATA(50 nm)/F_2PA + 10 wt % $Ir(ppy)_3$ (20 nm)/F-TBB (20 nm)/Alq_3 (10 nm)/LiF (0.5 nm)/Al (device H), was fabricated. As Figure 8 shows, green emission with a peak at 518 nm originating from the iridium complex was observed with negligible contribution of the blue-violet emission from F_2PA (less than 0.1% in intensity). The results indicate that excitation energy transfer from F_2PA to $Ir(ppy)_3$ occurs efficiently and that the device exhibits high performance. Figure 9 shows the voltage dependencies of

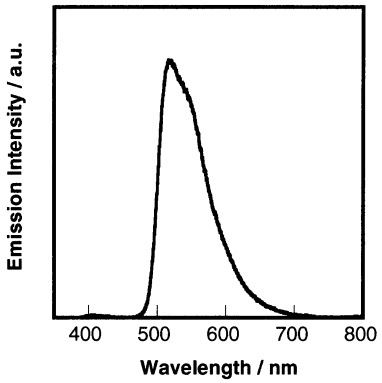

Figure 8. EL spectrum of phosphorescent organic EL device H, ITO/*m*-MTDATA (50 nm)/F_2PA + 10 wt % Ir(ppy)$_3$ (20 nm)/F-TBB (20 nm)/Alq$_3$ (10 nm)/LiF (0.5 nm)/Al.

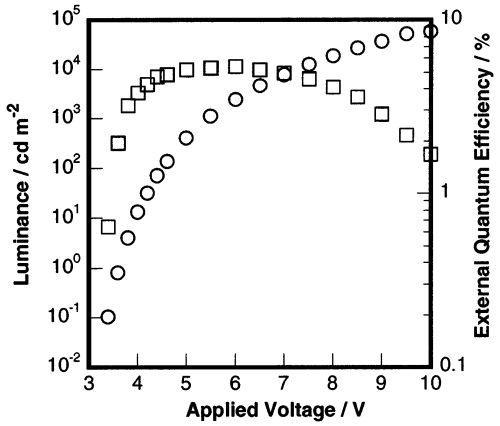

Figure 9. Luminance versus applied voltage (circle) and external quantum efficiency versus applied voltage (square) characteristics for phosphorescent organic EL device H, ITO/*m*-MTDATA (50 nm)/F_2PA + 10 wt % Ir(ppy)$_3$ (20 nm)/F-TBB (20 nm)/Alq$_3$ (10 nm)/LiF (0.5 nm)/Al.

luminous and external quantum efficiencies for the organic EL device H. The maximum luminous and external quantum efficiencies of the device H were 12.3 lm W^{-1} at a luminance of 72 cd m^{-2} and 5.4% at a luminance of 2500 cd m^{-2}, respectively. The maximum luminance was 56 900 cd m^{-2} at 10.0 V. The external quantum efficiency of the present device showed a small decrease as luminance increased, but an external quantum efficiency of 4.0% was still obtained at a luminance of 20 000 cd m^{-2}. The present study shows that the new amorphous molecular material F_2PA functions not only as a good blue-violet emitter but also as a good host material for the phosphorescent dopant Ir(ppy)$_3$.

Conclusions

A novel class of hole-blocking amorphous molecular materials, TBB, F-TBB, TFB, and TFPB, were designed and synthesized. They are characterized by high oxidation potentials and large HOMO−LUMO energy gaps. They readily form stable amorphous glasses with well-defined T_gs. These materials were found to function as good hole blockers for use in organic EL devices. The use of TBB, F-TBB, and TFPB as hole blockers in organic EL devices permitted efficient blue-violet emissions from amorphous molecular materials with hole-transporting properties, F_2PA, TPD, *p*-BPD, and PFFA. The fabricated devices exhibited high performance with low turn-on voltages from 3 to 5 V and high external quantum efficiencies from 1.08 to 1.95%. In addition, F_2PA was proven to function as a good host material for the phosphorescent dopant Ir(ppy)$_3$ as well as a blue-violet emitter in the presence of the hole-blocking layer of F-TBB.

The present study presents a new guideline for the molecular design of amorphous molecular materials that function as hole blockers for organic EL devices.

CM020849+